Journal of Applied Polymer Science

Evaluation of a Nanocomposite Hydrogel for Water Shut-Off in Enhanced Oil Recovery Applications: Design, Synthesis, and Characterization

Paul Tongwa, Runar Nygaard, Baojun Bai
Department of Geological Sciences and Engineering, Missouri University of Science and Technology , Rolla, Missouri 65409
Correspondence to: B. Bai (E-mail: baib@mst.edu)

ABSTRACT: This work involves the synthesis of a nanocomposite hydrogel from just polymer and clay without the use of conventional organic crosslinkers. Conventional hydrogel design usually involves a multicomponent reaction that incorporates monomer (or polymer), initiator, and an organic crosslinker. However, because of the many limitations, setbacks, and inconsistencies involved with organic crosslinkers, authors herein present a nanocomposite hydrogel that incorporates polymer and clay only. It was found that these hydrogels show surprising mechanical toughness, tensile moduli, and tensile strengths. Study of gel behavior reveal physical interaction between polymer and clay, due in part to adsorption of polymer chains onto clay surface and ionic interactions between anionic carboxylate groups of polymer chains and positive clay surface. X-ray diffraction patterns and Scanning Electron Microscopy revealed the formation of intercalated and exfoliated clay morphology. Increase in clay concentration and gel strength had a direct proportionality. The effect of clay concentration on hydrogel decomposition temperature was also reported by thermogravimetric analysis. © 2012 Wiley Periodicals, Inc.† J. Appl. Polym. Sci. 000: 000–000, 2012

KEYWORDS: gels; nanocomposites; nanoparticles; nanowires and nanocrystals; nanolayers; hydrogels

Received 5 December 2011; accepted 15 June 2012; published online
DOI: 10.1002/app.38258

INTRODUCTION

Excess water production is a frequent problem that occurs in mature reservoirs as a result of long-term water flooding. Such excess water production usually results in increased environmental concerns, increased levels of corrosion and scale, and ultimately leads to early shut-in of wells that still contain significant volumes of hydrocarbons.[1,2] In an attempt to mitigate excess water production and hence increase hydrocarbon production, hydrogels are often injected near wellbore to preferentially seal higher permeability zones or fractures, thus diverting injection water into low permeability unswept hydrocarbon-rich zones. Hydrogels are three-dimensional hydrophilic polymers, which in contact with water swell but do not dissolve as a result of a chemical or physical crosslinking and often than not will undergo a volume phase change when surrounding conditions such as temperature, salinity or pH change.[3] For many decades, hydrogels have been used in cosmetics and medicine,[4] agriculture,[5] and to address excess water production problems during enhanced oil recovery operations.[6–13] Most recently however, chemically crosslinked polymer-clay nanocomposites[14–19] have attracted great interests, both in industry and academia due mainly to the improvement in materials properties brought about by the incorporation of these nanomaterials. Shibayama et al.[20] and Haraguchi et al.[21,22] have reported an increase in hydrogel properties such as increased mechanical toughness and deformability and high heat resistance.

Mindful of the toxicity, environmental concerns, and the potential pollution of groundwater and private wells by downhole chemicals, the need to mitigate chemical usage in enhanced oil recovery operations is unavoidable. For this reason, our nanocomposite hydrogel was designed with just natural clays, without the utilization of conventional chemical crosslinkers. In addition, the cost of such chemical crosslinkers far supercedes natural clays. Furthermore, size exclusion chromatographic problems usually arise during injection. Due to significant differences in the molecular weights of polymer compared to crosslinker, crosslinkers tend to travel faster than polymers during downhole deployment, such that an uneven ratio of polymer/crosslinker occurs at near wellbore, thereby altering the original gelant composition and hence forming gels with less mechanical performances than expected. Thus, for these several limitations, the use of chemically crosslinked hydrogels is restricted. It is for these reasons that our current research proposes a nanocomposite hydrogel involving just polymer and clay without the

Applied Polymer SCIENCE

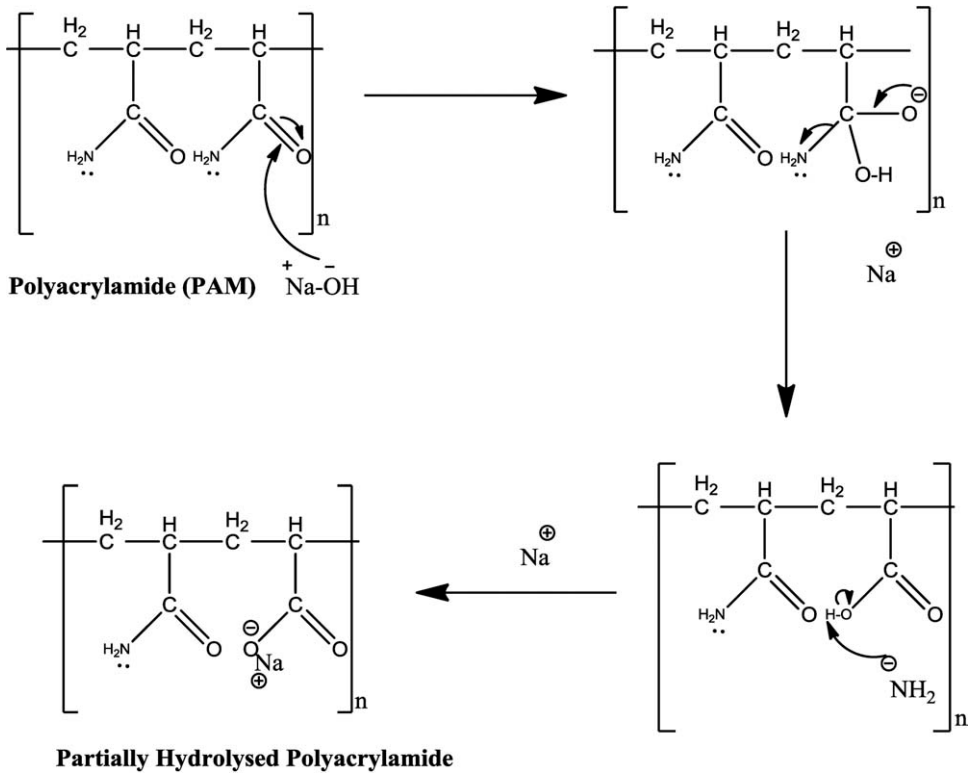

Scheme 1. Mechanism of alkaline hydrolysis of PAM to partially hydrolyzed PAM (HPAM).

incorporation of organic crosslinkers. The objective and novelty of the current work involve developing a facile physical crosslinking to prepare polyacrylamide (PAM)-based nanocomposite gels with significantly improved mechanical properties for the potential application in enhanced oil recovery.

Laponite is a synthetic layered silicate that has been used in a wide variety of applications including surface coatings, agriculture, personal care, and oil field applications.[23] A disk shaped crystalline colloid with an aspect ratio of ca. 27 nm (disk diameter ca. 25 nm and thickness of ca. 0.92 nm). It has a chemical formula $Na^{+}_{0.7}[(Si_8 Mg_{5.5} Li_{0.3}) O_{20}(OH)_4]^{-0.7}$. The crystal surface is negatively charged while the edges of the crystal have positive charges.[24] It is classified as an inert compound that is not degraded by high temperature or high shear dispersion processes. Hence, as a nanomaterial, it will impart thixotropy, improve stability and syneresis, and act as multifunctional physical crosslinks.PolyacrylamidePAMs on the other hand are water soluble, anionic polymers that have been extensively used in the petroleum industry because of their high viscous ability and affordability. They are synthesized by a free radical polymerization reaction of acrylamide monomer units. Subsequent alkaline hydrolysis converts the neutral amide groups of the polymer backbone into anionic carboxylate groups (Scheme 1). Their viscous power and chemical properties depend on the degree of hydrolysis (DH) and molecular weight.

EXPERIMENTAL

Materials and Methods

Anionic partially HPAM with an average molecular weight of 18 million and a DH of 30% was provided by SNF company (Andrezieux, France) under the trade name FLOPAAM 3630 S. HPAM was received as a white granular solid with a bulk density of ca. 0.75 ± 0.15 and is completely water soluble. As with most polymers, this contains about 10% moisture. Nanoclay used in this study, Laponite XLG was received with courtesy from Southern Clay Products Inc (Gonzales, Texas). All reagents were used as received. All solutions used in this experiment were prepared in 1% NaCl brine. NaCl brine was used as the solvent because this is the predominant salt found in reservoir (formation) water. We intend to mimic reservoir environment. At 1% NaCl concentration, electrostatic interaction between brine electrolytes and HPAM is negligible to prevent HPAM–XLG interaction.

The following nanocomposite hydrogel compositions (Table I) were prepared according to the following steps: First, the polymer powder was gradually added to the brine solvent with continuous stirring using a magnetic stirring bar for ca. 20 min to obtain a clear viscous solution. In a separate high shear Oster 16

Table I. Composition of Samples

Sample	HPAM mass % (mass fraction)	Laponite XLG mass % (mass fraction)
XLG1	0.8	1
XLG3	0.8	3
XLG5	0.8	5
XLG7	0.8	7
XLG10	0.8	10

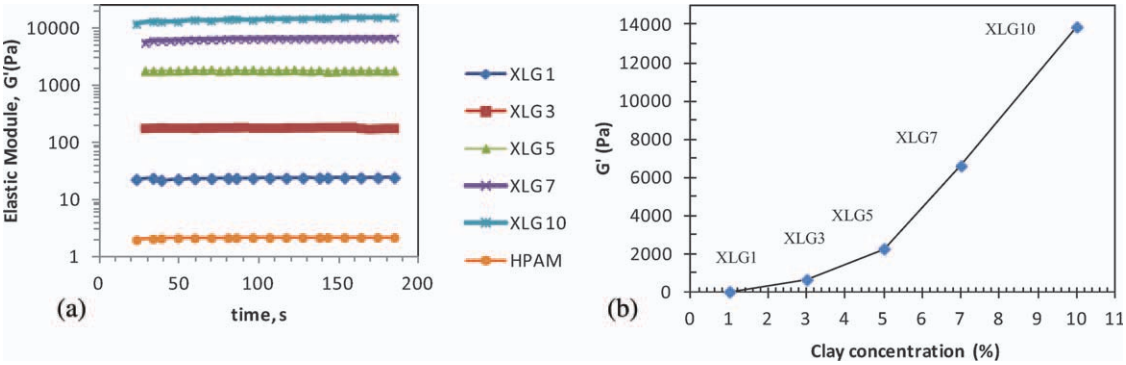

Figure 1. (a) Elastic moduli for hydrogel XLG1–10 and HPAM. (b) Increase in elastic module of XLG1–10 with clay concentration. [Color figure can be viewed in the online issue, which is available at wileyonlinelibrary.com.]

speed blender (at high switch and frappe speed), the corresponding amount of Laponite XLG particles were blended in 1% NaCl brine solution for 15–20 mins to ensure complete exfoliation. Then, separately dissolved HPAM solution was added to clay dispersion with continuous blending for an additional 5 min to obtain nanocomposite gel. Polymer concentration was kept at 8000 ppm (0.8%) while clay amounts were varied to study the effects of clay on nanocomposite gel strength. After this, product was cut into smaller sizes, put in petri dishes, and dried in oven at 40°C overnight for further characterization.

Characterization

To evaluate the degree of clay exfoliation and determine polymer intercalation between clay layers, small angle X-ray diffraction (XRD) was carried out using a Cu-Kα radiation (λ_1 = 1.5405; λ_2 = 1.5444) under a voltage of 45 kV and current of 40 mA. XRD patterns were obtained in 2θ ranges from 1 to 40° with a step size of 1.33°.

Differential Scanning Calorimetry (DSC) measurements to obtain glass transition temperatures (T_g) were performed using a DSC Q2000 series from TA Instruments in a nitrogen atmosphere with milled NC dried gel, heating from 25 to 400°C at a heating rate of 10°C/min.

Fourier Transform Infrared (FTIR) spectra were obtained from the conventional pressed KBr pellet method containing about 1.5% of dried gel using an FTIR-720 spectrophotometer.

Thermogravimetric analysis (TGA) was performed on dried gels with a sample size of ca. 22 mg using a TGA Q50 from TA Instruments. Samples were heated from 25 to 1000°C at a heating rate of 10°C/min.

Scanning electron microscope model S-4700 of Hitachi Company was used to observe the morphology of the prepared NC hydrogel. Dried samples were used.

The rheological properties of hydrogels were measured using a Haake RheoScope RO1 version 3.61.0000 from Thermo Scientific. The sensor used for all measurements was PP20 with a gap of 2 mm. The samples were cut in uniform dimensions with diameter of 2 cm and height of 2 mm. The measurements were set as an oscillation model and frequency experiments were first performed in the range of 1–15 Hz to establish the extent of the linear viscoelastic region. Based on the data, all subsequent oscillation time-dependent experiments were performed at a fixed frequency of 1 Hz and controlled stress of 1.0 Pa to obtain the values of G' and G'' as a function of time. All runs were repeated at least three times.

RESULTS AND DISCUSSION

Results

Rheological Behavior. The gelation behavior of XLG1–10 were studied. The mechanical strength of a gel often can be estimated by its viscoelastic properties such as elastic module (G') and viscous module (G''). The variation in elastic modulus (G') with time for nanocomposite gel XLG 1–10 is presented in Figure 1(a) and is compared against uncrosslinked polymer. It is observed from this figure that the elastic module significantly increases with increasing clay concentration, suggesting the existence of strong interactions between anionic polymer chains and positively charged clay rims. On the contrary, the elastic module for uncrosslinked polymer is at lowest value of 2 Pa. The clay nanoparticles are fixed in the gel network as additional effective junction points. A plausible mechanism for such polymer–clay interactions will be the adsorption of the polymer to the clay surface by hydrogen bonding between the oxygen atoms of clay and the amide protons of the polymer as well as the complex formation between metal ions on clay surface with carbonyl oxygen of the polymer. Furthermore, an increase in elastic module at high clay concentrations is due to clay network formation owing to the considerable clay layer interactions at high clay amounts. Figure 1(b) illustrates the increase in G' with clay concentration for nanocomposite gel XLG1–10.

Variations of elastic and viscous module for XLG1 and XLG10 with angular frequency are plotted in Figure 2(a) and (b). As shown in Figure 2(a), a medium gel is formed with an elastic module of ca. 30 Pa and the differences between G' and G'' increase progressively. However, in Figure 2(b), a strong gel is formed with an elastic module of ca. 30,000 Pa. The differences between G' and G'' remain almost constant. Thus, moving from XLG1 to XLG10, we observed an increase in elastic module of ca. 30,000 Pa. Such results further validate the increase of gel strength with clay concentration. Additional corroborations substantiating our results are presented in Figure 2(c). A small steady increase in gel strength is observed from XLG1 to 3,

Applied Polymer SCIENCE

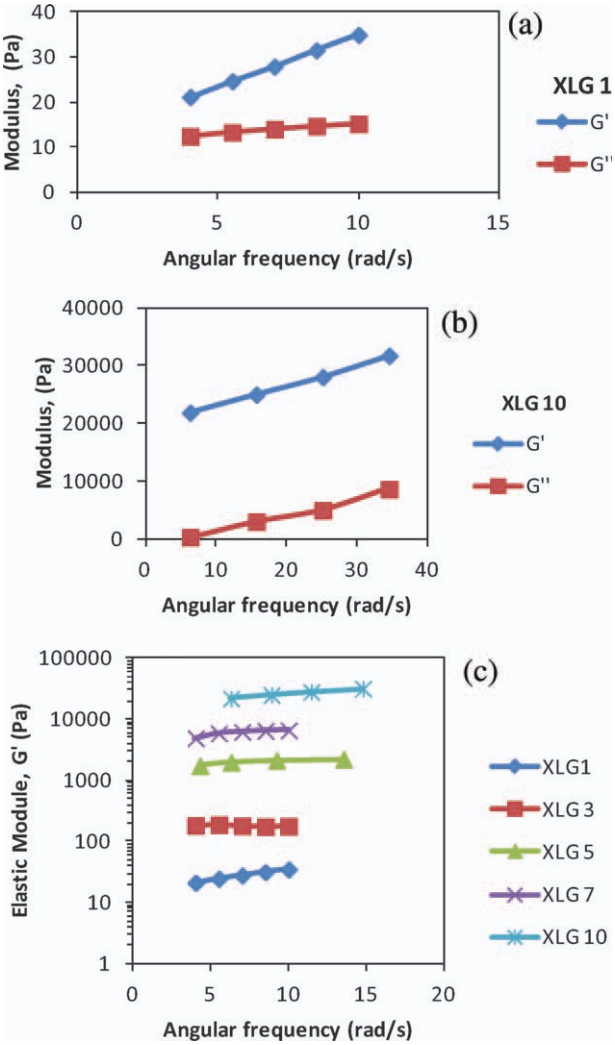

Figure 2. Variation of elastic (G') and viscous (G'') module with angular frequency for (a) nanocomposite gel XLG1, (b) XLG10, and (c) effects of clay concentration on nanocomposite gel strength for XLG1–10. [Color figure can be viewed in the online issue, which is available at wileyonlinelibrary.com.]

which increases further in XLG5. From XLG7 to 10, gel strength increased by several orders of magnitude.

XRD Analysis. Figure 3 presents the XRD patterns of Laponite XLG and nanocomposite gel XLG1–10. Intercalated or exfoliated clay morphologies are usually identified by monitoring the position of the basal reflection in the clay nanomaterial. In an exfoliated nanocomposite, an extensive separation of layers occurs such that the basal reflection disappears. However, in intercalated nanocomposites, a limited separation of layers occurs which results in a shift in basal reflection to a lower value. We observe a d_{001} interplanar distance in laponite XLG at $2\theta = 7.4°$ After incorporation of polymer, intercalated morphologies are observed in nanogels XLG3–10, as is evidenced by the shift of 2θ to lower angles which implies an increase in d spacing of clay (from Braggs equation; $n\lambda = 2d\sin\theta$). Complete exfoliation was observed for XLG1 as evidenced by the absence of the basal peak. This is due perhaps to the lower clay concentration. Similar results have been published by Zolfaghari et al.[25]

TGA and DSC Evaluation. TGA pattern of dried gel sample (XLG10) was evaluated and compared against uncrosslinked polymer. The thermogram of pure polymer [Figure 4(a)] shows three main decomposition regimes appearing at 211, 272, and 413°C. The loss of water molecules can be observed as a gradual decomposition from onset to ca. 200°C. The first and second sharp peaks appearing at 211 and 272°C can be attributed to the thermal decomposition of the amide and carboxylate side groups of the polymer chain, respectively.[26] Further heating to about 413°C results in another weight loss, which is suggested to be the decomposition of the polymer backbone.[27] However, when the polymer is crosslinked with clay, we observe a remarkably different thermogram [Figure 4(b)]. The first peak around 100°C is attributed to unbound water molecules. The sharp weight loss of the amide and carboxylate side groups not only reduced but also extended to 232 and 465°C. The decomposition peak of the amide side group at ca. 232°C is almost insignificant, possibly suggesting a complete decomposition of this group. The last peak at 675°C represents a remarkable extension of the polymer backbone decomposition temperature when crosslinked with clay. Thus, we observe a remarkable increase in thermal resistance of nanocomposite gel compared with uncrosslinked polymer confirming its application in high temperature reservoir environments.

Figure 5 presents the thermograms from DSC measurements for polymer and dried nanocomposite gel XLG1–10. In an attempt to determine the existence of flexible polymer chains in nanocomposite gel samples, DSC measurements were used to measure the thermal molecular motion of samples by observing shifts in T_g as clay concentration increases. It is known from literature that crosslinking increases T_g by introducing restrains

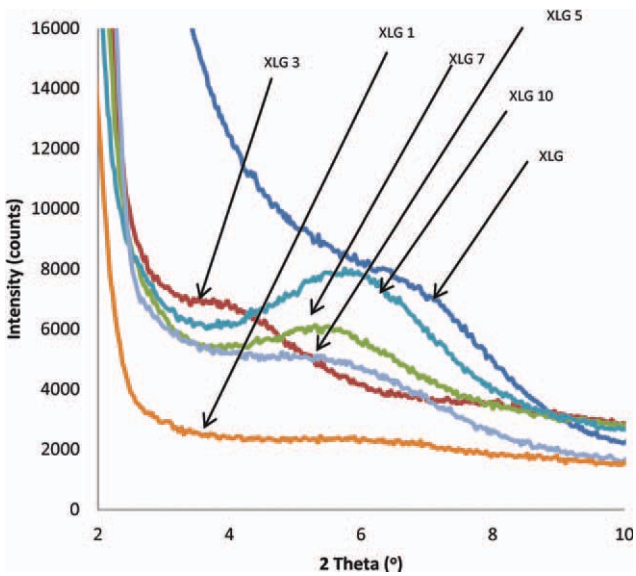

Figure 3. XRD patterns for clay (XLG) and dried gels (XLG1–10). [Color figure can be viewed in the online issue, which is available at wileyonlinelibrary.com.]

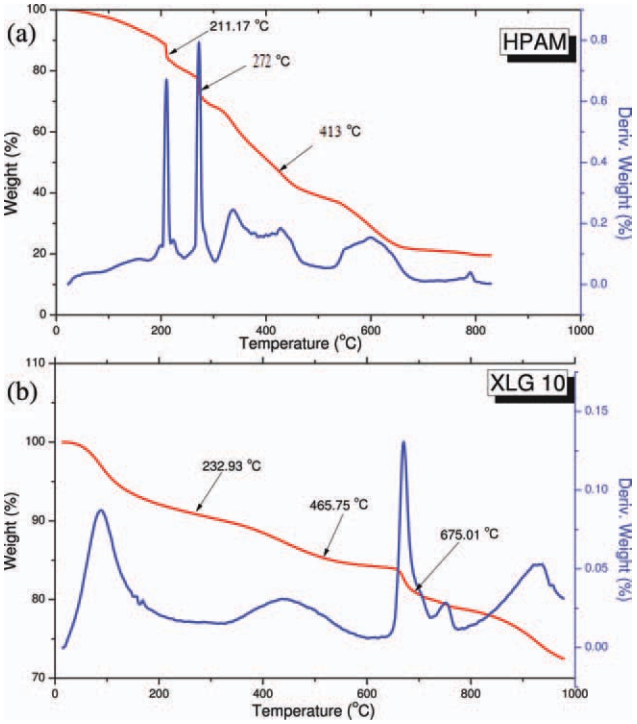

Figure 4. (a) Thermogravimetric (TG) patterns of uncrosslinked polymer (HPAM) and (b) 10% clay nanocomposite gel (XLG10). TGA was run at a rate of 10°C/minute from room temperature to 1000°C. [Color figure can be viewed in the online issue, which is available at wileyonlinelibrary.com.]

on the molecular motions of a chain. And such was our observation. In hydrogels, T_g was observed to gradually increase as crosslinker (clay) concentration increased. In addition, the transition also increasingly became broader with increase in clay concentration. Such observations affirm an increasing restraint in molecular motion with increasing clay content. T_g for uncrosslinked polymer was 108°C. This value increased to 117°C at 1% clay content. A steady increase to 161 and 168°C was observed when nanoclay concentrations were increased to 5 and 10%, respectively. Such results confirm the existence of a strong polymer–clay interaction. Thus, enhanced mechanical properties were realized in nanocomposite hydrogel.

FTIR Analysis. FTIR spectra of uncrosslinked polymer (HPAM), clay and XLG 10 nanocomposite gel were analyzed to investigate the changes in polymer molecular structure before and after crosslinking. The FTIR spectra of uncrosslinked polymer, clay, and XLG10 nanocomposite gel are presented in Figure 6. The weak intensity band of 3356 and 3183 cm^{-1} observed in HPAM undoubtedly refers to the presence of moisture as is common with most dried polymers. A similar band at 3393 and 3467 cm^{-1} observed in XLG10 also signifies the presence of unremoved water molecules (O—H) in gel sample during drying process. The strong intensity band at 3457 cm^{-1} observed in clay signifies the many O—H stretching vibrations present. Moving down to lower frequencies, the medium C=O stretching (amide) vibrations of HPAM occur at 1666 cm^{-1}, the corresponding band in XLG10 is a weak band at 1674 cm^{-1}. This indicates that the amide groups are still present in the two samples. This is consistent with results obtained by Murugan et al.[28] C=O stretching (carboxylate) is at 1565 cm^{-1}. The

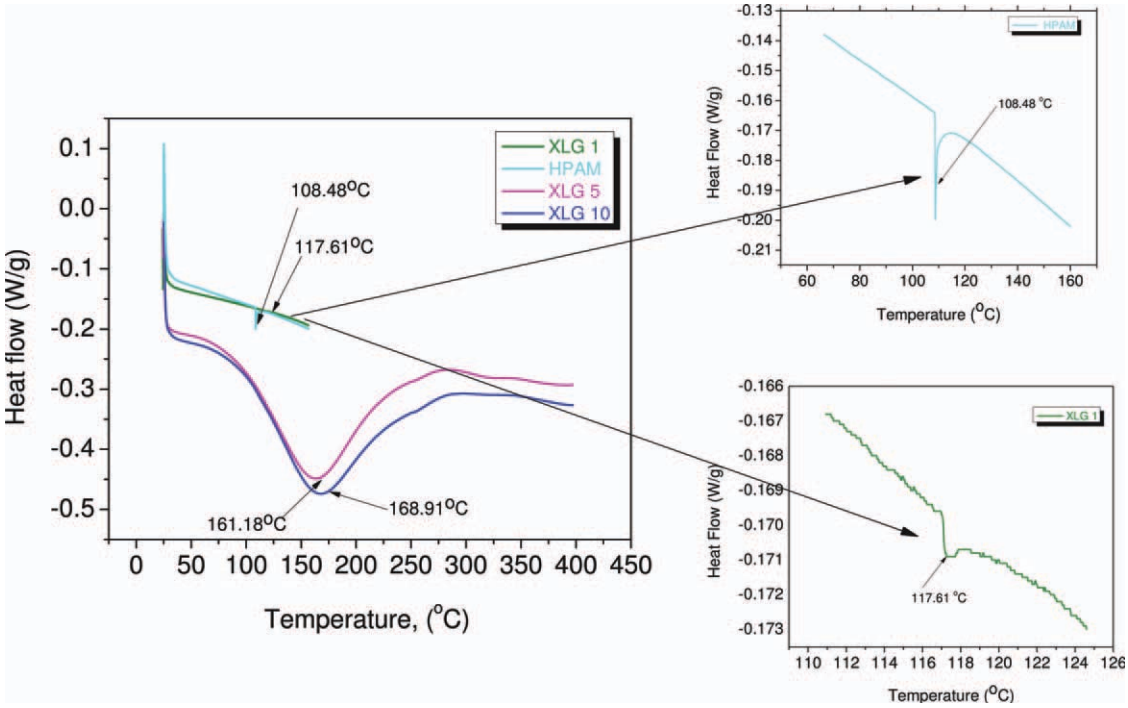

Figure 5. DSC thermograms for HPAM, XLG1, XLG5, and XLG10. Samples were heated at a rate of 10°C/minute. Thermograms for HPAM and XLG1 are magnified for clarity. [Color figure can be viewed in the online issue, which is available at wileyonlinelibrary.com.]

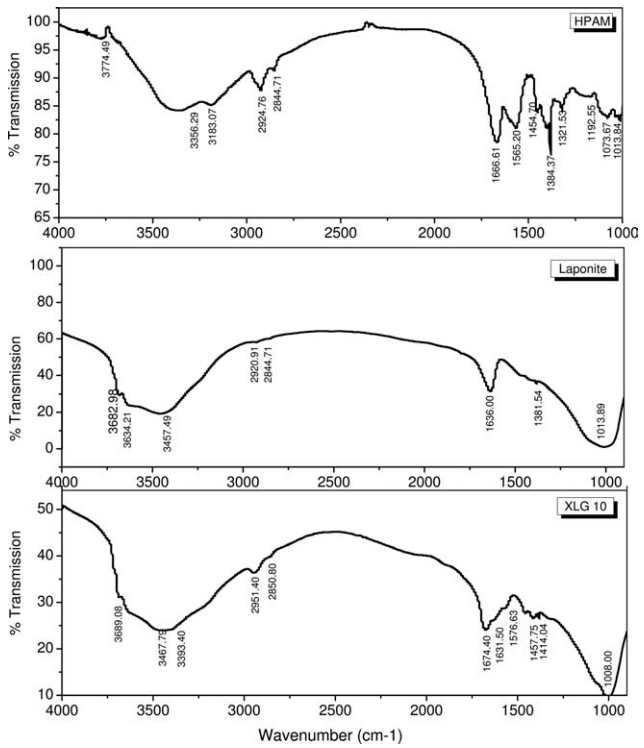

Figure 6. FTIR spectra of HPAM, laponite XLG, and nanocomposite gel XLG10.

difference in intensity in the amide bands in HPAM and XLG10 is due to their contribution in intermolecular hydrogen bonds with OH groups of clay. The CH_2 asymmetric and symmetric stretching vibrations at 2924 and 2844 cm^{-1} observed in HPAM remain almost unchanged in nanocomposite gel sample (2920 and 2844 cm^{-1}). The medium intensity band observed at 1426 cm^{-1} in HPAM has been assigned to C—N stretching (amide) vibrations.[29] The medium band at 1454 cm^{-1} has been assigned to NH_2 (amide) bending. The weak bands at 1073 and 1013 cm^{-1} refer to the C—C stretching vibrations.

Thus the vibrational assignments of HPAM and XLG 10 are discussed. No remarkable differences in spectra are observed, except for decrease in intensity in hydrogel bands particularly in region between 1100 and 1700 cm^{-1}, which is associated with intermolecular hydrogen bond interactions between polymer and clay.[28]

Scanning Electron Microscopy Analysis. Scanning electron microscopy (SEM) of HPAM was studied and compared against dried nanocomposite hydrogel XLG10. HPAM is seen as single particles in Figure 7(a) which after interaction with nanoclays form a dense and compact gel structure [Figure 7(b), arrows], thus suggesting a strong polymer–clay interaction.

DISCUSSION

In prior experiments, several unsuccessful attempts were made to disperse polymer in clay by simple magnetic stirring. Anionic HPAM has a surface negative charge due to its carboxylate (COO^-) group. The surface and edges of laponite XLG are negatively and positively charged, respectively. Thus, in solution, electrostatic attraction between edges and surface of different clay discs (rim–face interactions) causes the formation of tactoids or "house of cards," preventing adequate dispersion of clay in solution and hence inadequate intercalation of polymer in clay network. Several considerations were made to chemically modify the surface charges of the clay, making both surface and edge negatively charged, and thereby favor clay–clay repulsion and hence obtain better clay dispersion in solution. However, a negatively charged surface/edge clay will repel negatively charged polymer, thus gel formation will be impossible [Figure 8(a)]. After further consideration, authors finally settled on the utilization of a high shear mixer, which provides sufficient energy to completely shear clay platelets apart, forming exfoliated nanostructures which form a temporary dispersion until polymer is introduced and crosslinking occurs forming three-dimensional gel network. To understand the behavior and characteristics demonstrated by nanocomposite gel, it is necessary that we postulate a mechanism illustrating the interaction between the

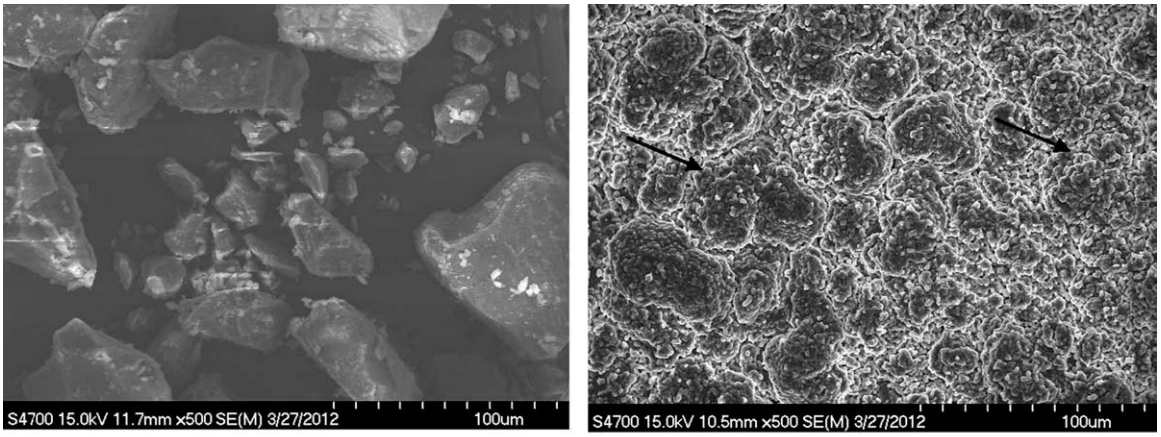

Figure 7. SEM of (a) HPAM and (b) XLG10. A dense and compact hydrogel is observed (as shown by the arrows), suggesting a strong polymer–clay interaction.

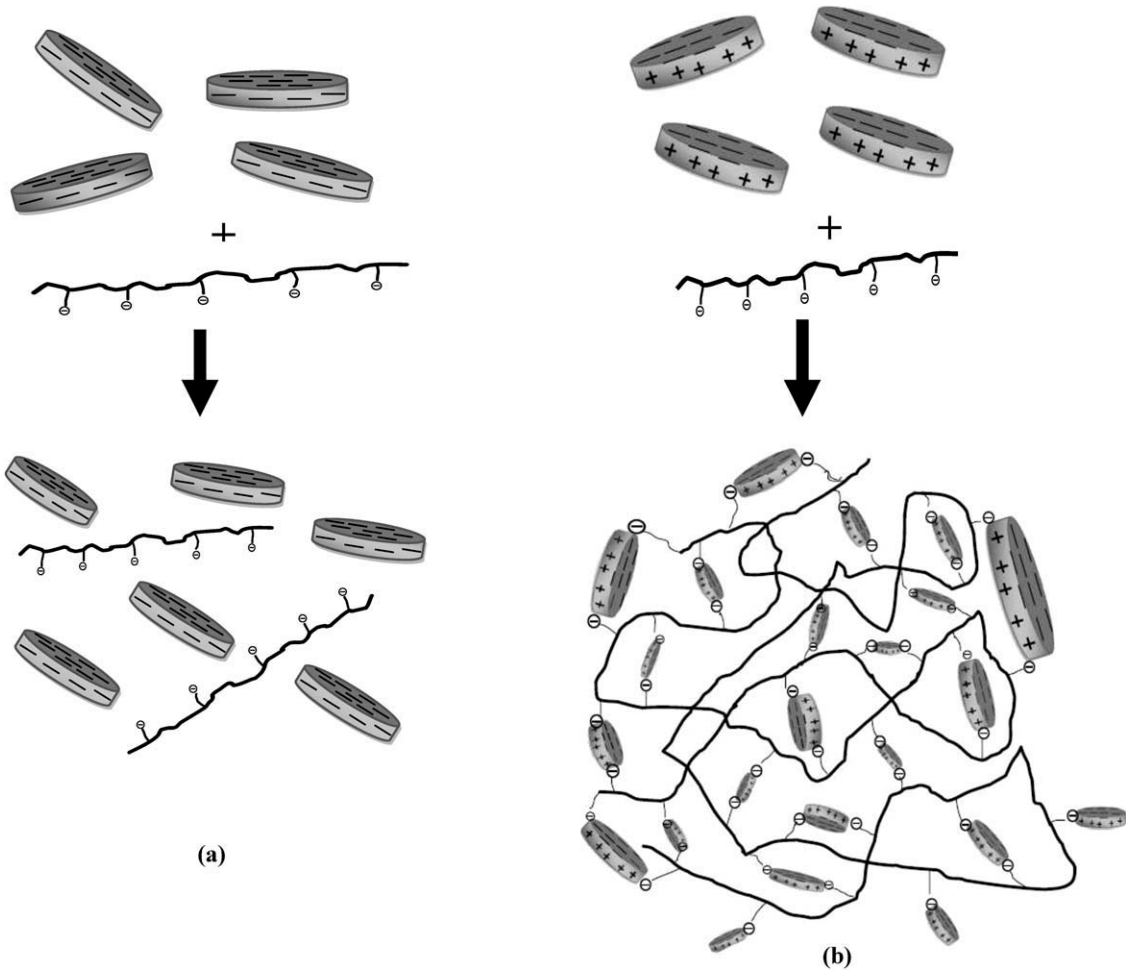

Figure 8. (a) Anionic–anionic polymer/clay repulsions results in no gelation. (b) Gelation occurs due to electrostatic interaction between anionic polymer and cationic clay surface.

polymer and clay [Figure 8(b)]. Based on our proposed model, the negatively charged polymer chains bind to the positively charged edges of the clay (polymer–rim interactions). This is further enhanced by the formation of hydrogen bond interactions between oxygen atoms in clay and hydrogen atoms in amide side chain of polymer (—$CONH_2$) as well as complexation of metal ions on clay surface with carboxylate oxygen atom of polymer (COO^-). As a consequence, nanocomposite gel exhibits remarkable mechanical performance suitable for use in control of excess water production through profile modification and as water shut-off agents during enhanced oil recovery operations.

CONCLUSIONS

1. A nanocomposite hydrogel synthesized by the reaction of polymer and clay was designed and characterized.
2. Small angle XRD revealed the formation of intercalated and exfoliated nanoclay structures.
3. TGA, DSC and FTIR spectroscopy revealed the formation of a hydrogel with remarkable mechanical toughness.
4. SEM revealed a dense hydrogel network, suggesting a strong polymer–clay interaction. Further confirmation was corroborated by rheology measurements. It was proven that gel strength had a direct proportionality with clay concentration.
5. The mechanical and rheological properties of these nanocomposite hydrogels suggest their application in high-temperature enhanced oil recovery applications.

ACKNOWLEDGMENTS

The authors gratefully acknowledge financial support from US Department of Energy's National Energy Technology Laboratory under grant # DE-FE0001132. An acknowledgement goes also to our project partner City Utilities of Springfield. Disclaimer: "This report was prepared as an account of work sponsored by an agency of the United States Government. Neither the United States Government nor any agency thereof, nor any of their employees, makes any warranty, express or implied, or assumes any legal liability or responsibility for the accuracy, completeness, or usefulness of any information, apparatus, product, or process disclosed, or represents that its use would not infringe privately owned rights. Reference herein to any specific commercial product, process, or service by trade name, trademark, manufacturer, or otherwise does not necessarily constitute or imply its endorsement, recommendation,

REFERENCES

1. Liu, Y.; Bai, B.; Shuler, P. J. Presented at the SPE/DOE Symposium on Improved Oil Recovery; Tulsa, OK, April 22–26, **2006.**
2. Bai, B.; Li, L.; Liu, Y.; Liu, H.; Wang, Z.; You, C. *SPE Reservoir Eval. Eng.* **2007,** *10*, 415.
3. Wen, F.; Sung, C. L. *J. Appl. Polym. Sci.* **2006,** *100*, 500.
4. Mahdavinia, G. R.; Zohuriaan, M. M. J.; Pourjavadi, A. *Polym. Adv. Technol.* **2004,** *15*, 173.
5. Pourjavadi, A.; Harzandi, A. M.; Hosseinzadeh, H. *Eur. Polym. J.* **2004,** *40*, 1363.
6. Bai, B.; Liu, Y.; Coste, J. P.; Li, L. *SPE Reservoir Eval. Eng.* **2007,** *10*, 176.
7. Bai, B.; Li, Y.; Liu, X. *Oil Drill. Prod. Technol.* **1999,** *20*, 3.
8. Bai, B.; Huang, F.; Liu, Y.; Seright, R. S.; Wang, Y. Presented at the 2008 SPE Improved Oil Recovery Symposium; Tulsa, OK, April 21–23, **2008.**
9. Liu, B.; Bai, B.; Li, Y. *Oil Drill. Prod.Technol.* **1999,** *21*, 3.
10. Zhang, H.; Bai, B. *SPE J.* **2011,** *16*, 388.
11. Vossoughi, S. J. *Pet. Sci. Eng.* **2000,** *26*, 199.
12. Wang, H. G.; Guo, W. K.; Jiang, H. F. Presented at the SPE International Symposium on Oilfield Chemistry; Houston, TX, February 13–16, **2001.**
13. Wang, W.; Liu, Y.; Gu, Y. *Colloid Polym. Sci.* **2003,** *281*, 1046.
14. Pavlidou, S.; Papaspyrides, C. D. *Prog. Polym. Sci.* **2008,** *33*, 1119.
15. Chung, Y. L.; Lai, H. M. *Carbohydr. Polym.* **2010,** *80*, 525.
16. Okay, O.; Oppermann, W. *Macromolecules* **2007,** *40*, 3378.
17. Darder, M.; Lopez-Blanco, M.; Aranda, P.; Leroux, F.; Ruiz-Hitzky, E. *Chem. Mater.* **2005,** *17*, 1969.
18. Darder, M.; Ruiz, A. I.; Aranda, P.; Van, D. H.; Ruiz, H. E. *Curr. Nanosci.* **2006,** *2*, 231.
19. Phang, I. Y.; Liu, T.; Mohamed, A.; Pramoda, K. P.; Chen, L.; Shen, L. *Polym. Int.* **2005,** *54*, 456.
20. Shibayama, M.; Suda, J.; Karino, T.; Okabe, S.; Takehisa, T.; Haraguchi, K. *Macromolecules* **2004,** *37*, 9606.
21. Haraguchi, K.; Takeshita, T. *Adv. Mater.* **2002,** *14*, 1121.
22. Haraguchi, K.; Takeshita, T.; Fan, S. *Macromolecules* **2002,** *35*, 10162.
23. Muller, F.; Salonen, A.; Glatter, O. *J. Colloid Interface Sci.* **2010,** *342*, 392.
24. Mongondry, P.; Tassin, F. R.; Nicolai, T. *J. Colloid Interface Sci.* **2005,** *283*, 397.
25. Zolfaghari, R.; Katbab, A. A.; Nabavizadeh, J.; Tabasi, R. J.; Nejad, M. H. *J. Appl. Polym. Sci.* **2006,** *100*, 2096.
26. Mathakia, I.; Vangani, V.; Pakshit, A. K. *J. Appl. Polym. Sci.* **1998,** *69*, 217.
27. Tutas, M.; Saglam, M.; Yuksel, M.; Guler, C. *Thermochim. Acta.* **1987,** *111*, 121.
28. Murugan, R.; Mohan, S.; Bigotto, A. *J. Korean Phys. Soc.* **1998,** *32*, 4, 505.
29. Kagöz, H.; Özgümü, S.; Orbay, M. *Polymer* **2001,** *42*, 7497.